MATERIAL GRADING FOR IMPROVED AEROELASTIC STABILITY
IN COMPOSITE WINGS

Liviu Librescu and Karam Y. Maalawi

MATERIAL GRADING FOR IMPROVED AEROELASTIC STABILITY IN COMPOSITE WINGS

LIVIU LIBRESCU AND KARAM Y. MAALAWI

A novel analytical formulation has been developed for the aeroelastic design of a class of solid nonuniform composite wings with improved aeroelastic torsional stability. Rectangular, unswept slender configurations made of unidirectional fibrous composites are considered, where the mechanical and physical properties can vary in the spanwise direction. Such a structural configuration yields to grading of the material properties along the wing span. The enhancement of the wing torsional stability can be attained, among others, by increasing the critical flight speed at which flutter or divergence instabilities occur. In this study, the latter problem is addressed, where the wing divergence speed is maximized while maintaining the total structural mass at a value equal to that of a known baseline design. Both continuous and discrete structural models have been examined, using classical elasticity and aerodynamic strip theories. The functional behavior of the divergence speed is comprehensively investigated by varying the volume fraction of the constituent materials in preassigned distributions. Exact solutions were obtained for different categories of unidirectionally reinforced composite wing structures: the linear volume fraction (L-VF), the parabolic volume fraction (PR-VF) and the piecewise volume fraction (PW-VF) wing models.

Our results reveal that in general, the torsional stability of the wing can be substantially improved by using nonuniform, functionally graded composites instead of the traditional ones having uniform volume fractions of the constituent materials. Several solutions are given for determining the optimal in-plane fiber distributions, which maximize the divergence speed of a wing made of carbon/epoxy composites without violating the performance requirements imposed on the total structural weight of the aircraft.

1. Introduction

Aeroelastic instabilities are a crucial factor in the design of modern flight vehicle structure. Friedmann [1999] demonstrated that several important aeroelastic problems are still far from being understood. Furthermore, the emergence of new technologies, such as the use of advanced composites and smart materials have invigorated aeroelasticity, and generated a host of new and challenging research topics that can have a major impact on the design of new generation of aerospace vehicles. The creative use of composite materials is becoming important for controlling aeroelastic instabilities beside the benefits of saving structural weight and increasing the fatigue life as well. For example, in the design of a laminated composite wing, Weisshaar [1987] and Karpouzian and Librescu [1994] showed that aeroelastic tailoring can be achieved commonly by varying the ply thickness, ply material and the stacking sequence. Another new class of composite materials can be produced by varying the volume fractions of their constituents in

a predetermined profile. Such nonuniform composites are called *functionally graded materials* (FGMs), in which the properties are functions of the spatial coordinates. Although the concept of aeroelastic tailoring of flight structures has been considered extensively in the literature [Librescu and Song 1992], functional grading has not yet, been implemented, to the authors' knowledge, in the available works. The main aim of the present paper is to open the door for the subject of aeroelastic tailoring of FGMs flight structures. The application to the optimization aspects in composite rotor blades [Ozbay et al. 2005] would also be a future extension of the current material grading concept.

Basic knowledge on the use of FGMs and their wide applications are given in [Suresh and Mortensen 1998]. FGMs were primarily used in situations where large temperature gradients are encountered and have also found several applications in the semiconductor industry. It was also shown that better performance for both static and dynamic behavior of structures fabricated from such advanced composite materials can be substantially achieved. There are different scenarios in modeling the spatial variation of material properties of a functionally graded structure. For example, Chen and Gibson [1998] performed experimental and theoretical analyses to determine the in-plane fiber distribution in unidirectional reinforced composites. They considered distributions represented by polynomial functions, and applied Galerkin's method to calculate the required polynomial coefficients from the resulting algebraic equations. Finally, they found that the linear variation of the volume fraction is a best fit with that predicted experimentally for selected composite beam specimens. Chi and Chung [2006] studied the mechanical behavior of FGM plates under transverse loading, where a constant Poisson's ratio and variable moduli of elasticity throughout the plate thickness was assumed. The volume fraction of the constituent materials were defined by simple power- laws, and closed form solutions using Fourier series were given for the case of simply- supported plates.

Considering structural stability of functionally graded beams, Elishakoff and Rollot [1999] presented closed-form solutions of the buckling load of a variable stiffness column. The modulus of elasticity was taken as a polynomial of the axial coordinate along the column's length. Cases in which a fourth-order polynomial serves as an exact buckling mode were provided. Another work dealing with the buckling behavior of two dimensional FGM rectangular plates subjected to in-plane edge loads was addressed by Chen and Liew [2004]. They applied a mesh-free approach, which approximates displacements based on a set of scattered nodes instead of the commonly implemented finite elements. Elishakoff and Guede [2004] then derived other closed-form solutions for the natural frequencies of an axially graded beam with variable mass and stiffness properties along its length.

In the field of the optimum design of FGM-structures, Qian and Batra [2005] considered frequency optimization of a cantilevered plate with variable volume fraction according to simple power-laws. They implemented genetic algorithms to find the optimum values of the power exponents, which maximize the natural frequencies, and concluded that the volume fraction needs to be varied in the longitudinal direction of the plate rather than in the thickness direction. More recently, Goupee and Vel [2006] proposed a methodology to optimize the natural frequencies of functionally graded beam with variable volume fraction of the constituent materials in the beam's length and height directions. They used a piecewise bicubic interpolation of volume fraction values specified at a finite number of grid points, and applied a genetic algorithm code to find the needed optimum designs.

As it clearly appears, in spite of its enormous potential benefits in aerospace industry, the use of the in-plane grading was exploited in problems involving only fundamental mechanical problems. The

same conclusions were given in the extensive review paper by Birman and Byrd [2007]. In the present study, analytical solutions are developed and presented for improving the torsional stability of a slender subsonic wing through optimal grading of the material volume fraction in the spanwise direction. Three models have been thoroughly analyzed: continuous linear (L-VF), continuous parabolic (PR-VF) and piecewise (PW-VF) mathematical models. The enhancement of the wing torsional stability is measured by maximization of the divergence speed while maintaining the total structural mass at a value equals to that of a known baseline design. The functional behavior of the divergence speed is comprehensively investigated by varying the volume fraction of the constituent materials in preassigned distributions. Enhanced wing designs made-up from carbon/epoxy composite material have been obtained and discussed. Side constraints are set on the fiber volume fractions to not exceed prescribed lower and upper limiting values.

## 2. Statement of the problem and basic formulation

When the flight speed of an aircraft exceeds a certain value called the divergence speed, V_{div}, the aerodynamic twist moment applied to the wing exceeds the restoring elastic moment of its structure [Bisplinghoff and Ashley 1962]. This causes static torsional instability of the lifting surface, which may twist to failure. Therefore, high divergence speed can be regarded as a major aspect in designing an efficient lifting surface with enhanced torsional stability. Maximization of the divergence speed can also have other desirable effects on the overall structural design. It helps in avoiding the occurrence of large displacements, distortions and excessive vibrations, and may also reduce fretting among structural parts, which is a major cause of fatigue failure. Consider an unswept, slender wing with rectangular planform and solid cross section, as depicted in Figure 1. The coordinates x_1 and x_2 are associated with the wing middle surface, whereas the x_3-axis points in the airfoil thickness direction. In the present model formulation, the wing is considered to be made of unidirectional fiber-reinforced composites with variable fiber volume fraction in the spanwise direction, x_1. The flow is taken to be steady, and incompressible. The aspect ratio is assumed to be sufficiently large with no major cutouts through the structure so that the classical engineering theory of torsion can be applicable and the state of deformation described in terms of one space coordinate. The elastic axis is assumed to be well defined and, hence, the bending and torsion degrees of freedom can be decoupled. For wings with low aspect ratio, the cross section warping ought to be included to account for three dimensional deformation effects [Librescu and Thangjitham 1991]. This will be considered by the authors in an extension of the present study.

It was shown by in [Lekhnitski 1981, Chapter 6, Sections 55–56] and [Tsai et al. 1990] that the equivalent shear modulus G of a unidirectionally reinforced composite lamina with thin cross section can be determined from the relation

$$G = f_1 G_{12},$$

where f_1 is a function that depends on the geometry and thickness ratio h/C of the cross section (C being the chord length and h the maximum thickness of the cross section) and on the ratio G_{12}/G_{13} between the in-plane and out-of-plane shear moduli G_{12} and G_{13}.

For many types of fibrous composites commonly utilized in aircraft structures, such as carbon/epoxy and graphite epoxy, the two moduli are approximately equal. Some experimental results were given in [Tsai and Daniel 1990] for the determination of the in- and out-of-plane shear moduli. We apply here
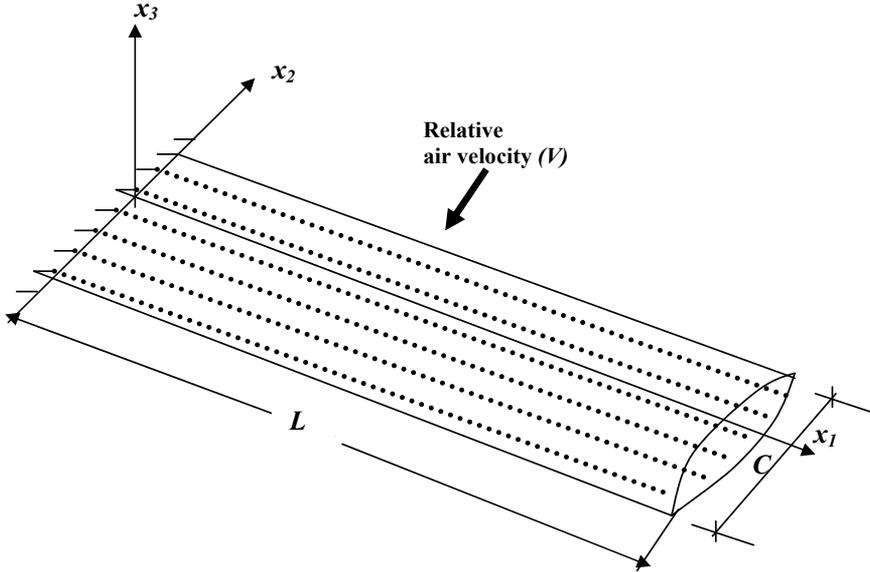
Figure 1. Unidirectional fiber-reinforced composite wing model.

semiempirical formula from [Halpin and Tsai 1967] to determine G_{12}:

$$G_{12} = G_m \frac{1 + \xi \eta V_f}{1 - \eta V_f}, \quad \text{where} \quad \eta = \frac{(Gf/Gm) - 1}{(Gf/Gm) + \xi}, \tag{1}$$

where G_m and G_f ($\equiv G_{f12}$, in the x_1-x_2 plane) are the shear moduli of the matrix and fiber materials, V_f is the fiber volume fraction and the parameter ξ is called the reinforcing efficiency and may be taken as 100% for theoretical analysis [Daniel and Ishai 2006]. The variation of the fiber volume fraction in FGM structures is usually described by power-law or exponential function models:

$$\begin{aligned} V_f(x) &= V_{fr}(1 - \beta x^p), & \beta &= (1 - \Delta), \\ V_f(x) &= V_{fr} e^{\beta x}, & \beta &= \ln \Delta, \end{aligned} \tag{2}$$

where $\Delta = V_{ft}/V_{fr}$ is the ratio between the fiber volume fractions V_{ft} and V_{fr} at the wing tip and at the root, the symbol $x = x_1/L$ denotes the dimensionless spanwise coordinate and p is an integer exponent. Wings with uniform, linear or parabolic distributions of $V_f(x)$ correspond to $p = 0$, 1 and 2. Similar distributions were utilized in [Chi and Chung 2006] to analyze FGM plates under transverse loading. The exponential distribution is not considered in the present investigation.

3. Stability analysis

Using classical elasticity and aerodynamic strip theories, we can write the differential equation governing wing torsional stability (see [Bisplinghoff and Ashley 1962]) as

$$\frac{d}{dx_1}\left(GJ\frac{d\alpha}{dx_1}\right) + \tfrac{1}{2}\rho V^2 C^2 ea\alpha(x_1) = 0, \tag{3}$$

subject to the boundary conditions

$$\alpha(0) = 0 \quad \text{for } x_1 = 0,$$

indicating that the elastic angle of attack α vanishes at the wing root, and

$$\left[GJ \frac{d\alpha}{dx_1} \right]_{x_1=L} = 0 \quad \text{for } x_1 = L,$$

which says that the torsional moment T vanishes at the wing tip. Here J is the torsion constant, which for thin wings with solid cross section, is directly proportional to the cube of the maximum airfoil thickness h, and the chord length C:

$$J = f_2 C h^3,$$

where f_2 is a shape factor that depends upon the geometry of the airfoil section. The other parameters in (3) are defined as follows: ρ is the air density, depending on the flight altitude, V is the flight speed, e is the fractional location of the shear center, positive aft with respect to the aerodynamic center, and a is the airfoil lift-curve slope.

It is convenient to normalize all variables and parameters with respect to a baseline design having uniform mass and stiffness distributions. The baseline is made of a uniform unidirectional fibrous composite with equal volume fraction of the matrix and fiber materials: $V_{f0} = 50\%$. The optimum wing designs presented herein shall have the same material type of construction, wing planform geometry, airfoil section, and same total structural mass as those of the baseline design. Therefore, the preassigned parameters ought to be selected as the type and dimensions of the airfoil section (that is, C, J, e and a are fixed), wing span L, and type of material of construction (that is, G_m, G_f, ρ_m, ρ_f are fixed). The flight altitude is also fixed (that is, ρ is fixed). Therefore, the only remaining variable to be taken into consideration is the distribution of the modulus of rigidity in the spanwise direction. Normalizing with respect to the uniform baseline design defined above, (3) takes the dimensionless form

$$(\hat{G}\alpha')' + \hat{V}^2 \alpha(x) = 0, \quad \alpha(0) = 0, \quad \alpha'(1) = 0, \tag{4}$$

where $\hat{G} = G_{12}/G_{12,0}$ is the dimensionless shear modulus and the prime denotes differentiation with respect to the dimensionless coordinate $x = x_1/L$. The dimensionless flight speed is defined by

$$\hat{V} = VCL\sqrt{\frac{\rho e a}{2GJ_0}},$$

where GJ_0 is the torsional stiffness of the baseline design. The shear modulus $G_{12,0}$ of the baseline design can be calculated from (1) by setting $V_{f0} = 0.5$ and $\xi = 1$. Substituting Equations (1) and (2) into (4), we get

$$(1 - f^2)\alpha'' + 2f'\alpha' + \mu(1 - f)^2 \alpha = 0, \tag{5}$$

where

$$f = \eta V_f(x) \quad \text{and} \quad \mu = \hat{V}^2 \frac{2 + \eta}{2 - \eta}.$$

3.1. *Continuous model: An exact power series solution.* Since f is a polynomial, an exact power series solution to (5) can be obtained by the method of Frobenius [Edwards and Penney 2004], in which the general solution is expressed as

$$\alpha(x) = \sum_{m=1}^{2} C_m \lambda_m(x),$$

where the C_m are constants of integration and the λ_m are two linearly independent solutions having the form

$$\lambda_m(x) = \sum_{n=m}^{\infty} a_{m,n} x^{n-1}, \quad m = 1, 2.$$

The unknown coefficients $a_{m,n}$ can be determined by substitution into the differential equation (5) and equating coefficients of like powers of x. The required recurrence formulas have been evaluated and are given for the linear distribution model by

$$a_{m,n} = \frac{2\beta\gamma(n-2)\big(1-\gamma(n-3)\big)a_{m,n-1} + \big((n-3)(n-4)(\beta\gamma)^2 - \mu(1-\gamma)^2\big)a_{m,n-2} - 2\beta\gamma\mu(1-\gamma)a_{m,n-3} - \mu(\beta\gamma)^2 a_{m,n-4}}{(n-1)(n-2)(1-\gamma^2)}$$

and for the parabolic distribution model by

$$a_{m,n} = \frac{\big(2\beta\gamma(n-3)(2-\gamma(n-4)) - \mu(1-\gamma)^2\big)a_{m,n-2} + \big((\beta\gamma)^2(n-5)(n-6) - 2\beta\gamma\mu(1-\gamma)\big)a_{m,n-4} - \mu(\beta\gamma)^2 a_{m,n-6}}{(n-1)(n-2)(1-\gamma^2)},$$

where $\gamma = \eta V_{fr}$. A coefficient $a_{m,n}$ is set equal to zero whenever n is less than m, and the leading coefficients $a_{m,m}$ in each series are arbitrary and can be set to one. This method was successfully applied by Maalawi and Negm [2002] to determine the exact rotating frequencies of a wind turbine blade in flapping motion.

Application of the associated boundary conditions and consideration of the nontrivial solution lead to the required characteristic equation:

$$\lambda_2'(1) = 0,$$

which is to be solved for the lowest root corresponding to the critical flight speed $\hat{V}_{\text{div}}$ at which divergence of the wing occurs.

3.2. *Piecewise wing model.* A piecewise model concept was used by [Maalawi 2002] to find optimized designs of elastic columns against buckling. The optimization variables included the cross section dimensions as well as the length of each segment composing the column, and several solutions were given for both solid and tubular configurations. It was concluded that the use of piecewise models in structural optimization gives excellent results and can be promising for similar applications. Figure 2 shows a rectangular lifting surface, which is constructed from N uniform piecewise panels, each of which has different fiber volume fractions and length. For the k-th panel (see Figure 3), Equation (4) reduces to

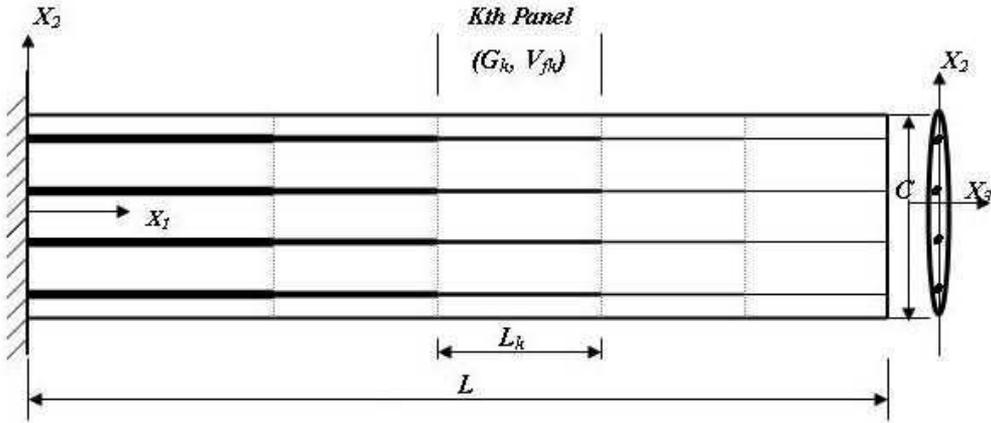$$\alpha''(\hat{x}) + \lambda_k^2 \alpha(\hat{x}) = 0, \qquad \lambda_k = \hat{V}/\sqrt{\hat{G}_k}, \tag{6}$$

Figure 2. Rectangular lifting surface constructed from piecewise panels: wing planform geometry
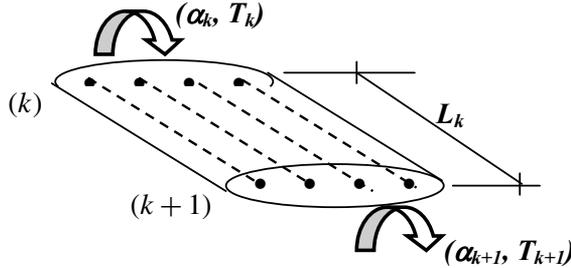.

Figure 3. Definition of the state variables for the k-th panel.

where $\hat{x} = x - x_k$ is a local coordinate, ranging from 0 to $\hat{L}_k = L_k/L$, the dimensionless length of the k-th panel, and $\hat{G}_k$ is the dimensionless shear modulus of the kth wing panel.

The exact solution of (6) is of course

$$\alpha(\hat{x}) = A\sin(\lambda_k\hat{x}) + B\cos(\lambda_k\hat{x}),$$

where A and B are the constants of integration. The dimensionless internal torsional moment, $T(\hat{x})$, can be obtained by differentiating this equation and multiplying by the dimensionless torsional rigidity:

$$T(\hat{x}) = \hat{G}_k\alpha' = \lambda_k\hat{G}_k\big(-A\sin(\lambda_k\hat{x}) + B\cos(\lambda_k\hat{x})\big).$$

Applying the boundary conditions at stations k and $k+1$ (see Figure 3), we obtain at $\hat{x} = 0$ the equations

$$\alpha_k = A, \quad T_k = B\lambda_k\hat{G}_k, \tag{7}$$

and at $\hat{x} = \hat{L}_k$ the equations

$$\alpha_{k+1} = A\cos(\lambda_k\hat{L}_k) + B\sin(\lambda_k\hat{L}_k),$$
$$T_{k+1} = \lambda_k\hat{G}_k\big(-A\sin(\lambda_k\hat{L}_k) + B\cos(\lambda_k\hat{L}_k)\big). \tag{8}$$

Substituting from (7) into (8), the relation between the state variables (α, T) at both ends of the k-th panel can be expressed by the matrix equation

$$\begin{Bmatrix} \alpha_{k+1} \\ T_{k+1} \end{Bmatrix} = E^{(k)} \begin{Bmatrix} \alpha_k \\ T_k \end{Bmatrix}, \quad \text{where} \quad E^{(k)} = \begin{bmatrix} \cos \lambda_k \hat{L}_k & \sin \lambda_k \hat{L}_k / (\lambda_k \hat{G}_k) \\ -\lambda_k \hat{G}_k \sin \lambda_k \hat{L}_k & \cos \lambda_k \hat{L}_k \end{bmatrix}.$$

It is now possible to compute the state variables progressively along the wing span by applying continuity requirements of the variables (α, T) among the interconnecting boundaries of the various wing panels. Therefore, the state variables at the extreme boundaries are related by the matrix equation

$$\begin{Bmatrix} \alpha_{N+1} \\ T_{N+1} \end{Bmatrix} = E \begin{Bmatrix} \alpha_1 \\ T_1 \end{Bmatrix}, \tag{9}$$

where

$$E = E^{(N)} E^{(N-1)} \dots E^{(3)} E^{(2)} E^{(1)}.$$

The nontrivial solution of equation (9) can be determined by applying the appropriate boundary conditions at the wing root and tip sections. The resulting transcendental equation, also named the characteristic equation, is given by

$$E_{22} = 0,$$

which can be solved for determining the critical flight speed at which torsional divergence instability occurs.

4. Results and discussion

The mathematical models developed in the previous sections have been applied to obtain wing designs with improved torsional stability, measured in the context of static aeroelasticity, by raising the divergence speed without weight penalties. The selected wing material is carbon-AS4 / epoxy-3501-6 composite, which has favorable characteristics and is highly desirable in both civilian and military aircraft structures. Its properties are given in Table 1. Lower and upper bounds of 25% and 75%, respectively are imposed on the fiber volume fraction. The total structural mass M is kept equal to the mass M_0 of the baseline design, so the dimensionless mass $\hat{M} = M/M_0$ equals 1. Since the fiber volume fraction of the baseline design, V_{f0}, equals 50%, a feasible design must satisfy the constraint equations

$$\int_0^1 V_f(x)\, dx = 0.5$$

for the continuous model or

$$\sum_{k=1}^N V_{fk} \hat{L}_k = 0.5 \tag{10}$$

for the piecewise model, where V_{fk} and $\hat{L}_k$ are the fiber volume fraction and dimensionless length of the k-th panel (Figure 2).

The mass density distribution $\rho_c(x)$ of the composite material is determined by the rule of mixture, assuming no voids are present:

$$\rho_c(x) = \rho_m + (\rho_f - \rho_m) V_f(x).$$

| Property	fiber	matrix
Mass density (g/cm^3)	$\rho_f = 1.81$	$\rho_m = 1.27$
Young's moduli (GPa)	$E_{1f} = 235$	$E_m = 4.3$
	$E_{2f} = 15$	
Shear moduli (GPa)	$G_{12f} = 27.0$	$G_m = 1.60$
	$G_{23f} = 7.0$	
Poisson's ratio	$\nu_{12f} = 0.2$	$\nu_m = 0.35$

Table 1. Material properties of carbon-AS4 / epoxy-3501-6 composite. The data are from [Daniel and Ishai 2006]. For a final structural design, however, experimental verifications are necessary.

The developed level curves of the dimensionless critical velocity $\hat{V}_{\text{div}}$ in V_{fr}-V_{ft} design space for the linear grading model (L-VF) are depicted in Figure 4, left. We see that $\hat{V}_{\text{div}}$ is a well behaved function and continuous in the design variables, namely, the fiber volume fractions at the wing root, V_{fr}, and tip, V_{ft}. It increases monotonically with the penalty of increasing the total structural weight, which has a harmful effect on the overall performance characteristics of the aircraft design. Therefore, maintaining the mass constant, one must follow the line $\hat{M} = 1$, as shown in the figure, to attain a feasible design. Results for the parabolic model (PR-VF) are depicted in Figure 4, right.

The variation of $\hat{V}_{\text{div}}$ and the fiber volume fraction at the wing root V_{fr} with the ratio $\Delta = V_{ft}/V_{fr}$ is given in Figure 5. Results for both linear and parabolic grading models are depicted, are based on the preservation of the total structural mass ($\hat{M} = 1.0$). As Δ increases, V_{div} decreases until it reaches its
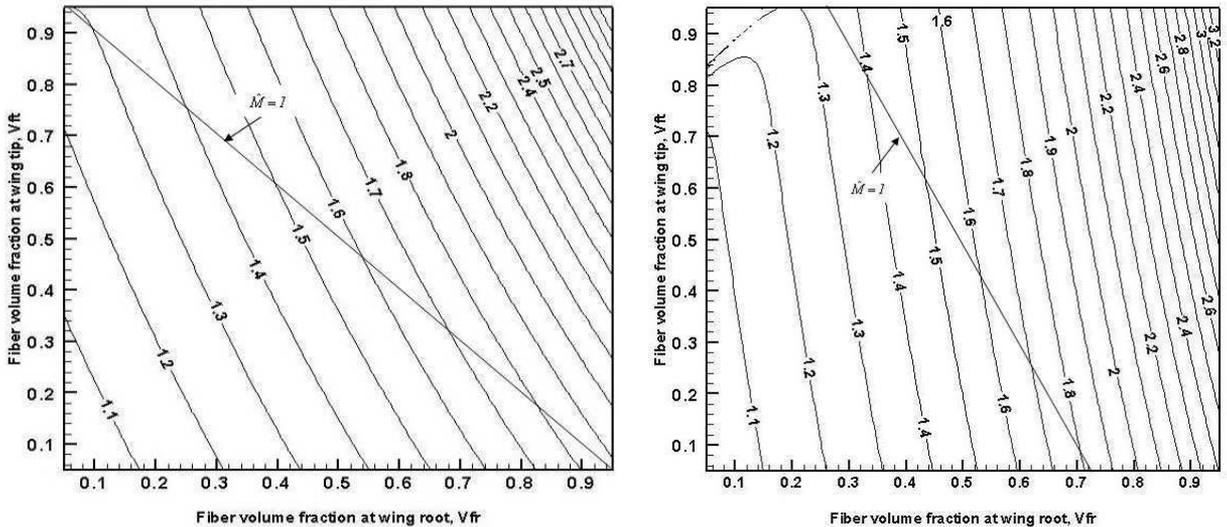
Figure 4. Isomerits of $\hat{V}_{\text{div}}$ in the V_{fr}-V_{ft} design space. Left: L-VF model. Right: PR-VF model.
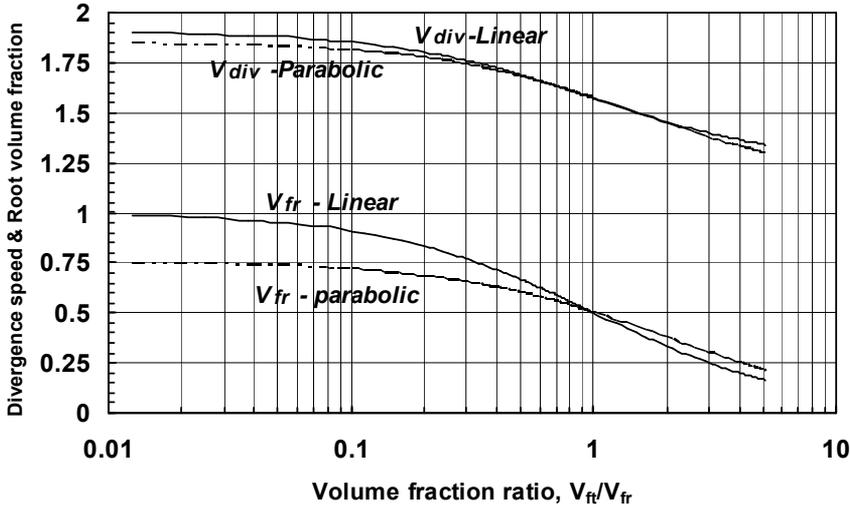
Figure 5. Variation of $\hat{V}_{\mathrm{div}}$ and V_{fr} with volume fraction ratio ($\hat{M} = 1.0$).

principal value $\pi/2$, which corresponds to the uniform baseline design having volume fraction of 50%. When Δ exceeds unity, a noticeable drop in the divergence speed occurs resulting in an undesirable degradation in the overall torsional stability level of the wing. Table 2 gives the final results for both cases with and without the side constraints imposed on $V_f(x)$.

It is observed that the linear grading excels the parabolic one in attaining higher torsional stability levels. However, this may not guarantee satisfactions of other strength requirements. The parabolic distribution seems to be more feasible since the main characteristic length of the fibers' cross section (say, the diameter of a circular fiber) can change linearly along the span.

We next consider the piecewise model (PW-VF). Figure 6, left, shows the developed isomerits for a wing composed from two panels. The design variables are $(V_{f1}, \hat{L}_1)$ and $(V_{f2}, \hat{L}_2)$. However, one of the panel lengths can be eliminated, because of the equality constraint $\hat{L}_1 + \hat{L}_2 = 1.0$. Another variable can also be discarded by applying the mass equality constraint (10), which further reduces the number of variables to only any two of the whole set of variables. The level curves shown in the figure represent the dimensionless critical speed $\hat{V}_{\mathrm{div}}$, augmented with the equality mass constraint, $\hat{M} = 1.0$. It is seen that

	L-VF		PR-VF	
	Case A	Case B	Case A	Case B
V_{fr}	1.0	0.75	0.75	0.625
Δ	0.0	0.33	0.0	0.4
$\hat{V}_{\mathrm{div}}$	1.91	1.75	1.85	1.71
Gain	21%	11%	18%	9%

Table 2. Carbon/epoxy wing designs with improved torsional stability ($\hat{M} = 1.0$). Case A: No side constraints are imposed on $V_f(x)$. Case B: The side constraint $0.25 \le V_f(x) \le 0.75$ is imposed. Gain is relative to the baseline value ($\pi/2$) of $\hat{V}_{\mathrm{div}}$.
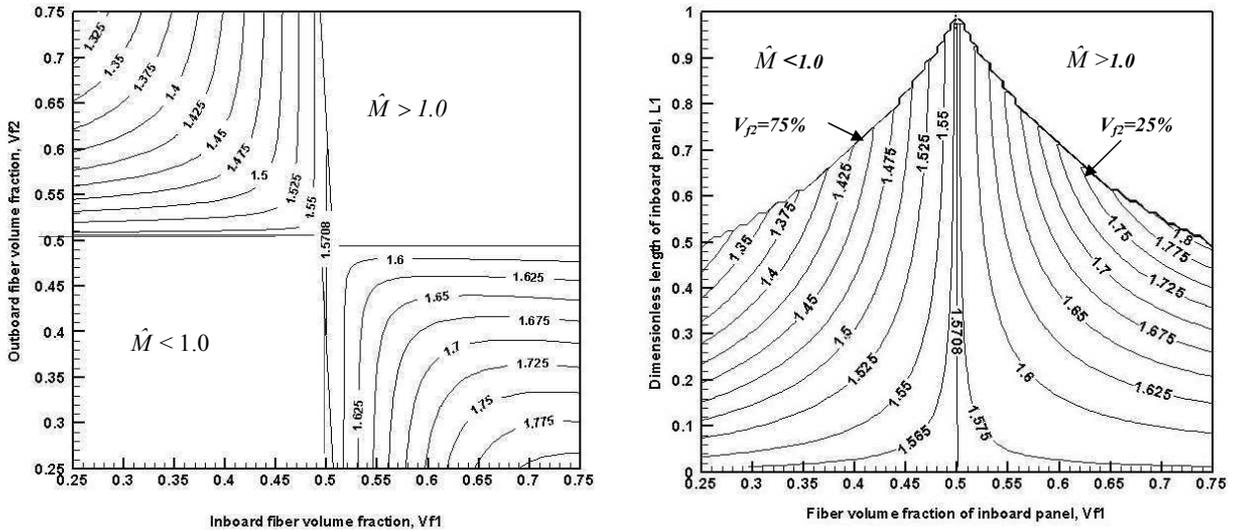
Figure 6. Isomerits of $\hat{V}_{\text{div}}$ in V_{f1}-V_{f2} design space (left) and V_{f1}-$\hat{L}_1$ design space (right) for a two-panel wing.

the function is well behaved and continuous everywhere in the selected design space V_{f1}-V_{f2}, except in the empty regions of the first and third quadrants, where the equality mass constraint is violated. The cross lines $V_{f1} = 0.5$ and $V_{f2} = 0.5$ represent the level curves of the principal value $\pi/2$.

The functional behavior of the divergence speed in the V_{f1}-$\hat{L}_1$ design space is shown in Figure 6, right. The shape of the contour lines resemble the streamlines of a flow originated from a jet at the vertex $(V_{f1}, \hat{L}_1) = (0.5, 1.0)$ and collides with a flat plat located at the horizontal line $\hat{L}_1 = 0$, with the stagnation point $(V_{f1}, \hat{L}_1) = (0.5, 0.0)$. The middle vertical line $V_{f1} = 0.5$ represents the contour of the principal value $\pi/2$ of the uniform baseline wing design. Two empty zones, where the equality mass constraint is violated, are indicated in the figure.

The feasible domain is bounded from above by the two curved lines representing the upper and lower limiting constraints imposed on the volume fraction of the outboard wing panel. The contours inside the feasible domain are not allowed to penetrate these borderlines and obliged to turn sharply to be asymptotes to them, in order not to violate the mass constraint. This is why they appear in the figure as zigzag lines.

The constrained optima were found to be $(V_{f1}, \hat{L}_1) = (0.75, 0.5)$ and $(V_{f2}, \hat{L}_2) = (0.25, 0.5)$, which means that the side constraints are always active [Venkataraman 2002].

The corresponding maximum value of the divergence speed is $\hat{V}_{\text{div}} = 1.81$, representing an optimization gain of 15%. This means that a piecewise grading of the material is slightly better than the parabolic model described by Equation (2). Isomerits of a three-panel wing is depicted in Figure 7, which has a pyramidal shape with its vertex at the design point $(V_{f2}, \hat{L}_2) = (0.5, 1.0)$ having $\hat{V}_{\text{div}} = \pi/2$ and $\hat{M} = 1.0$. The feasible domain is bounded from above by the two lines representing cases of a two-panel wing, with $V_{f1} = 0.75$ for the line to the left and $V_{f3} = 0.25$ for the right line. Both have a zigzag pattern because of the crowded pattern of the interior contours, which are forced to turn and becoming asymptotical to them, in order not to violate the mass equality constraint.
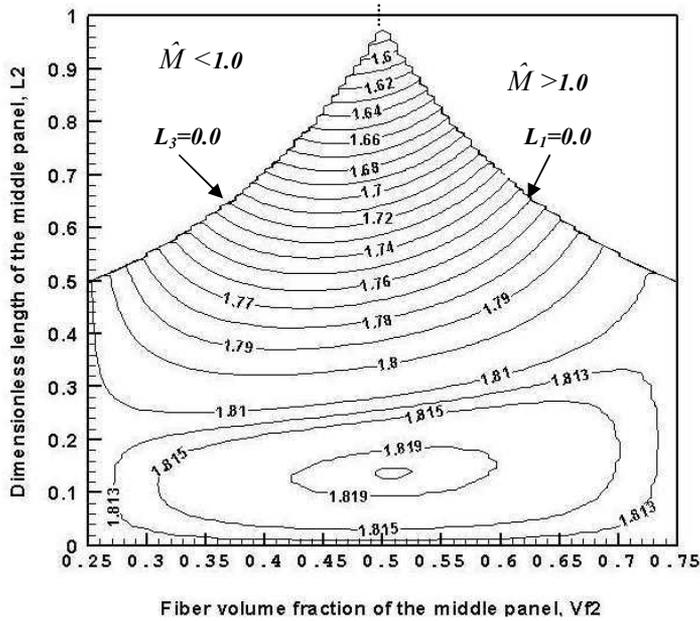
Figure 7. Global optimality solution for a three-panel wing model.

The final global optimal solution, lying in the bottom of the pyramid, can be calculated using the MATLAB optimization toolbox routines [Venkataraman 2002]. We obtain

$$(V_{f1}, \hat{L}_1) = (0.75, 0.43125), \quad (V_{f2}, \hat{L}_2) = (0.50, 0.1375), \quad (V_{f3}, \hat{L}_3) = (0.25, 0.43125), \quad \hat{V}_{\text{div}} = 1.82.$$

This represents an optimization gain of about 16%.

5. Conclusions

We have presented a novel design approach, based on the proper use of functional graded materials for improving the overall torsional stability of a class of unidirectionally reinforced composite wings. The torsional stability is measured by increasing the critical flight speed at which wing divergence occurs while not violating performance requirements imposed on the total structural weight of the aircraft. The mechanical and physical properties of the material are optimized in the spanwise direction, where the spatial distribution of the fiber volume fraction is assumed to be prescribed by either continuous or piecewise mathematical models. Lower and upper bounds are imposed on the design variables in order to avoid having odd-shaped optimized configurations with unrealistic values of the volume fractions. The functional behavior of the divergence speed $\hat{V}_{\text{div}}$ with the selected optimization variables has been thoroughly investigated, and useful design charts are given showing conspicuous design trends for wings with improved aeroelastic performance. The given exact mathematical approaches ensured the attainment of global optimality of the proposed wing model.

To our knowledge, aeroelastic tailoring of a wing with material grading in the spanwise direction had not yet been considered in the available research work. It has been the major aim of this paper to open the door for such a promising direction in the field of aeroelasticity of flight structures. Future work includes

aeroelastic optimization of functionally graded trapezoidal and swept wings. The behavior when grading is performed in both the spanwise and the airfoil thickness directions is now under study.

Acknowledgments

References

[Birman and Byrd 2007] V. Birman and W. L. Byrd, "Modeling and analysis of functionally graded materials and structures", *Applied Mechanics Reviews* (2007). to appear.

[Bisplinghoff and Ashley 1962] R. L. Bisplinghoff and H. Ashley, *Principles of aeroelasticity*, Wiley, New York, 1962.

[Chen and Gibson 1998] W.-H. Chen and R. F. Gibson, "Property distribution determination of non-uniform composite beams from vibration response measurements and Galerkin's method", *J. App. Mech.* **65** (1998), 127–133.

[Chen and Liew 2004] X. L. Chen and K. M. Liew, "Buckling of rectangular functionally graded material plates subject to nonlinearly distributed in-plane edge loads", *J. Smart Materials and Structures* **13** (2004), 1430–1437.

[Chi and Chung 2006] S.-H. Chi and Y.-L. Chung, "Mechanical behavior of functionally graded material plates under transverse load, I: analysis", *International Journal of Solids and Structures* **43** (2006), 3657–3674.

[Daniel and Ishai 2006] I. M. Daniel and O. Ishai, *Engineering mechanics of composite materials*, 2nd ed., Oxford Univ. Press, New York, 2006.

[Edwards and Penney 2004] C. H. Edwards and D. E. Penney, *Differential equations and boundary value problems: computing and modeling*, Prentice Hall, Englewood Cliffs, NJ, 2004.

[Elishakoff and Guede 2004] I. Elishakoff and Z. Guede, "Analytical polynomial solutions for vibrating axially graded beams", *J. Mech. Adv. Mater. Struct.* **11** (2004), 517–533.

[Elishakoff and Rollot 1999] I. Elishakoff and O. Rollot, "New closed-form solutions for buckling of a variable stiffness column by Mathematica", *J. Sound Vib.* **224** (1999), 172–182.

[Friedmann 1999] P. P. Friedmann, "Renaissance in aeroelasticity and its future", *J. Aircraft* **36** (1999), 105–121.

[Goupee and Vel 2006] A. J. Goupee and S. S. Vel, "Optimization of natural frequencies of bidirectional functionally graded beams", *Journal of Structural and Multidisciplinary Optimization* **32**:6 (2006), 73–484.

[Halpin and Tsai 1967] J. C. Halpin and S. W. Tsai, "Effects of environmental factors on composite materials", technical report AFML-TR-67-423, Dayton, OH, 1967.

[Karpouzian and Librescu 1994] G. Karpouzian and L. Librescu, "Comprehensive model of anisotropic aircraft wings suitable for aeroelastic analysis", *J. Aircraft* **31**:3 (1994), 703–712.

[Lekhnitski 1981] S. G. Lekhnitski, *Theory of elasticity of an anisotropic elastic body*, Mir, Moscow, 1981.

[Librescu and Song 1992] L. Librescu and O. Song, "On the static aeroelastic tailoring of composite aircraft swept wings modeled as thin-walled beam structures", *Composite Engineering* **2**:5 (1992), 497–512.

[Librescu and Thangjitham 1991] L. Librescu and S. Thangjitham, "Analytical studies on static aeroelastic behavior of forward-swept composite wing structures", *J. Aircraft* **28**:2 (1991), 151–157.

[Maalawi 2002] K. Y. Maalawi, "Buckling optimization of flexible columns", *Int. J. Solids Struct.* **39** (2002), 5865–5876.

[Maalawi and Negm 2002] K. Y. Maalawi and H. M. Negm, "Optimal frequency design of wind turbine blades", *J. Wind Engineering and Industrial Aerodynamics* **90**:8 (2002), 961–986.

[Ozbay et al. 2005] S. Ozbay, E. Armanios, O. Bauchau, and D. S. Dancila, "Extension-twist coupling optimization in composite rotor blades", in *Proceedings of the 46th AIAA/ASME/ASCE/AHS/ASC Structures, Structural Dynamics and Materials Conference* (Austin, TX, 2005), 2005.

[Qian and Batra 2005] L. F. Qian and R. C. Batra, "Design of bidirectional functionally graded plate for optimal natural frequencies", *J. Sound Vib.* **280** (2005), 415–424.

[Suresh and Mortensen 1998] S. Suresh and A. Mortensen, *Fundamentals of functionally graded materials*, Cambridge Univ. Press, 1998.

[Tsai and Daniel 1990] C. L. Tsai and I. M. Daniel, "Determination of inplane and out-of-plane shear moduli of composite materials", *J. Exper. Mech.* **30** (1990), 295–299.

[Tsai et al. 1990] C. L. Tsai, I. M. Daniel, and G. Yaniv, "Torsional response of rectangular composite laminates", *J. App. Mech.* **57** (1990), 383–387.

[Venkataraman 2002] P. Venkataraman, *Applied Optimization with MATLAB Programming*, Wiley, New York, 2002.

[Weisshaar 1987] T. A. Weisshaar, "Aeroelastic tailoring: Creative uses of unusual materials", technical report 87-0976, 1987.

LIVIU LIBRESCU: Deceased 16 Apr 2007
Department of Engineering Science and Mechanics, Virginia Polytechnic Institute and State University, 318 Norris Hall, Blacksburg, VA 24061, United States

KARAM Y. MAALAWI: maalawi@netscape.net
Department of Mechanical Engineering, National Research Center, 12622 Dokki, Cairo, Egypt